Supporting Information

Constructing Layered Structure Amidine-Based Pentazolate Salts with Low Sensitivity

Pengfei Wang[1], Lile Liu[1], Zebang Sun[1], Feng qin[1], Lei Shi[1], Chao gao[1], Yang Du[1], Chong Zhang[1] Bingcheng Hu[1] and Chengguo Sun[1,2] *

[1] School of Chemical Engineering, Nanjing University of Science and Technology, Nanjing, Jiangsu 210094, China;

[2] School of Chemical Engineering, University of Science and Technology Liaoning, Anshan, Liaoning, 114051, China;

E-mail: cgsun@njust.edu.cn

Contents

1. Experimental section.

Caution! Although the authors did not encountered difficulties in dealing with these energetic materials, some compounds in this study are extremely dangerous. Every step must be carried out on a small scale and according to the best safety practices such as wearing face shields and leather gloves.

1.1 Reagents and instruments

All reagents and solvents were purchased from MACKLIN and Aladdin as analytical grade and were used as received. TG and DSC plots were acquired on a simultaneous thermal analyzer (Netzsch STA449 F3) at a scan rate of 10 ℃/min^{-1} in perforated Al containers under a nitrogen flow of 50 mL /min^{-1}. IR spectra were recorded on a Bruker ALPHA II fourier transform infrared spectrometer. Mass spectrum analyses were carried out on a Thermo Scientific mass spectrometer. Powder X-ray diffraction (PXRD) measurements were performed on a Bruker D8 QUEST X-ray diffractometer using Mo Kα (λ=0.71073Å) radiation. Morphology scanning were performed under thermal field emission scanning electron microscope (Apreo s). Impact and friction sensitivity measurements were performed using a standard BAM Fallhammer and BAM friction tester. The 1H spectra were recorded on a 500MHz (Bruker AVANCE III 500) nuclear magnetic resonance spectrometer. Elemental analyses were performed on a vario EL III CHNOS elemental analyzer.

1.2 Computational methods

All enthalpy calculations were performed with the Gaussian09 (Revision D.01) suite of programs[1]. The geometric optimization, frequency analysis and single-point energies were accomplished at the B3LYP/6-311+G** level. The enthalpy of an isodesmic reaction was obtained by combining the B3LYP/6-311+G** energy difference for the reactions, the scaled zero point energies (ZPE), values of thermal correction (HT), and other thermal factors. The solid phase heat of formation was calculated based on the Born–Haber energy cycle according to the literature method. The NCI and ESP plots were calculated using Multiwfn and visualized using the VMD program[2-6]. Hirshfeld surfaces and associated 2D fingerprints were generated using CrystalExplorer17[7].

1.3 X-ray crystallography

The single-crystal X-ray diffraction measurements for all the compounds were conducted on a Bruker D8 QUEST diffractometer using Mo-Kα radiation (λ=0.71073Å) with a graphite monochromator at 150K or 293 K. An Oxford Cobra low temperature device was used to maintain the low temperature. Integration and scaling of intensity data were accomplished using the SAINT program. The structures were solved by intrinsic methods using SHELXT2018 and refinement was carried out by a full-matrix least-squares technique using SHELXL2018/3 Hydrogen atoms were refined isotropically, and the heavy atoms were refined anisotropically. N–H and O–H hydrogens were located from different electron density maps, and C–H hydrogens were placed in calculated positions and refined with a riding model. Data were corrected for the effects of absorption using SADABS. Relevant crystal data and refinement results are summarized in Table S1-S28.

1.4 Synthetic procedures

AgN_5 was synthesized according to our previous method.

Formamidine pentazolate (1): Dispersed 1.05 mmol of pentazolate silver salt in a mixed solution of methanol and water in a ratio of 9:1. Added 1.00 mmol of methanol solution of methylamine hydrochloride to the above mixed solution. The reaction was stirred at room temperature for 6 hours under dark conditions. Filtered to remove silver chloride precipitate, and dried the filtrate under reduced pressure to obtain a white solid. Yield:109.2 mg (0.95 mmol, 95%). Td (onset): 105 °C. IR:

$\tilde{\nu}$ = 3152, 3035, 1702, 1418, 1327, 1215, 1067, 655, 559 cm^{-1}. Raman: $\tilde{\nu}$ = 3037, 1674, 1413, 1170, 1124, 1064, 690, 563 cm^{-1}. m/z (ESI^+-MS): 44.83 $[M\text{-}N_5]^+$. IS: >40 J. FS: >360 N. 1H NMR (500 MHz, DMSO-d6) δ 8.74 (s, 4H), 7.77 (s, 1H). Elemental analysis (%) calcd. for CH_5N_7 (115.12): C, 10.44; H, 4.38; N, 85.18; found: C, 10.27; H, 4.03; N, 85.70.

Acetamidine pentazolate (2): Dispersed 1.05 mmol of pentazolate silver salt in a mixed solution of methanol and water in a ratio of 9:1. Added 1.00 mmol of methanol solution of methylamine hydrochloride to the above mixed solution. The reaction was stirred at room temperature for 6 hours under dark conditions. Filtered to remove silver chloride precipitate, and dried the filtrate under reduced pressure to obtain a white solid. Yield:120.0 mg (0.93 mmol, 93%). Td (onset): 116 °C. IR: $\tilde{\nu}$ = 3311, 3133, 2779, 1706, 1403, 1327, 1211, 1067, 997, 655, 552 cm^{-1}. Raman: $\tilde{\nu}$ = 1412, 1172, 1122, 1095, 1011, 565 cm^{-1}. m/z (ESI^+-MS): 59.11 $[M\text{-}N_5]^+$. IS: >40 J. FS: >360 N. 1H NMR (500 MHz, DMSO-d6) δ 2.00 (s, 3H), 9.10 (s, 2H), 8.62 – 8.58 (m, 2H). Elemental analysis (%) calcd. for $C_2H_7N_7$ (129.15): C, 18.60; H, 5.47; N, 75.93; found: C, 18.28; H, 5.63; N, 76.09.

Cyclopropane-1-carboximidamide pentazolate (3): Dispersed 1.05 mmol of pentazolate silver salt in a mixed solution of methanol and water in a ratio of 9:1. Added 1.00 mmol of methanol solution of methylamine hydrochloride to the above mixed solution. The reaction was stirred at room temperature for 6 hours under dark conditions. Filtered to remove silver chloride precipitate, and dried the filtrate under reduced pressure to obtain a white solid. Yield:145.8 mg (0.94 mmol, 94%). Td (onset): 122 °C. IR: $\tilde{\nu}$ = 3309, 3086, 2781, 1688, 1519, 1439, 1210, 1106, 924, 813, 755, 644, 565, 454 cm^{-1}. Raman: $\tilde{\nu}$ = 3026, 1530, 1436, 1339, 1194, 1172, 1040, 918, 815, 766, 566, 459 cm^{-1}. m/z (ESI^+-MS): 84.96 $[M\text{-}N_5]^+$. IS: >40 J. FS: >360 N. 1H NMR (500 MHz, DMSO-d6) δ 8.44 (d, J = 123.3 Hz, 4H), 1.77 (tt, J = 8.3, 5.1 Hz, 1H), 1.11 (dddd, J = 13.8, 11.4, 8.7, 4.2 Hz, 4H). Elemental analysis (%) calcd. for $C_4H_9N_7$ (155.18): C, 30.96; H, 5.85; N, 63.19; found: C, 31.22; H, 5.52; N, 63.26.

Benzamidine pentazolate (4): Dispersed 1.05 mmol of pentazolate silver salt in a mixed solution of methanol and water in a ratio of 9:1. Added 1.00 mmol of methanol solution of methylamine hydrochloride to the above mixed solution. The reaction was stirred at room temperature for 6 hours under dark conditions. Filtered to remove silver chloride precipitate, and dried the filtrate under reduced pressure to obtain a white solid. Yield:172.1 mg (0.90 mmol, 90%). Td (onset): 113 °C. IR: $\tilde{\nu}$ = 3077, 2024, 1677, 1603, 1523, 1471, 1219, 1086, 782, 683, 510 cm^{-1}. Raman: $\tilde{\nu}$ = 3075, 1608, 1532, 1483, 1179, 1032, 995, 766 cm^{-1}. m/z (ESI^+-MS):120.93 $[M\text{-}N_5]^+$. IS: >40 J. FS: >360 N. 1H NMR (500 MHz, DMSO-d6) δ 9.08 (s, 4H), 7.84 – 7.78 (m, 2H), 7.78 – 7.70 (m, 1H), 7.63 (t, J = 7.8 Hz, 2H). Elemental analysis (%) calcd. for $C_7H_9N_7$ (191.21): C, 43.97; H, 4.75; N, 51.28; found: C, 43.64; H, 4.59; N, 51.77.

1H-1,2,4-triazole-1-carboxamidine pentazolate (5): Dispersed 1.05 mmol of pentazolate silver salt in a mixed solution of methanol and water in a ratio of 9:1. Added 1.00 mmol of methanol solution of methylamine hydrochloride to the above mixed solution. The reaction was stirred at room temperature for 6 hours under dark conditions. Filtered to remove silver chloride precipitate, and dried the filtrate under reduced pressure to obtain a white solid. Yield:167.6 mg (0.92 mmol, 92%). Td (onset): 112 °C. IR: $\tilde{\nu}$ = 3384, 3120, 1718, 1657, 1532, 1394, 1282, 1223, 1132, 1095, 977, 872, 730, 659, 523, 461 cm^{-1}. Raman: $\tilde{\nu}$ = 3131, 1541, 1398, 1351, 1285, 1181, 1134, 1100, 977, 692, 465 cm^{-1}. m/z (ESI^+-MS): 111.84 $[M\text{-}N_5]^+$. IS: >40 J. FS: >360 N. 1H NMR (500 MHz, DMSO-d6) δ 9.68 (s, 4H), 9.36 (dd, J = 5.9, 2.3 Hz, 1H), 8.59 – 8.46 (m, 1H). Elemental analysis (%) calcd. for $C_3H_8N_{10}O$ (200.19): C, 18.00; H, 4.03; N, 69.98; O, 7.99; found: C, 18.33; H, 4.15;

N, 69.83; O, 7.69.

Malonamideamidine pentazolate (6): Dispersed 1.05 mmol of pentazolate silver salt in a mixed solution of methanol and water in a ratio of 9:1. Added 1.00 mmol of methanol solution of methylamine hydrochloride to the above mixed solution. The reaction was stirred at room temperature for 6 hours under dark conditions. Filtered to remove silver chloride precipitate, and dried the filtrate under reduced pressure to obtain a white solid. Yield:165.2 mg (0.96 mmol, 96%). Td (onset): 120 °C. IR: $\tilde{\nu}$ = 3067, 1663, 1398, 1274, 1216, 870, 748, 554 cm^{-1}. Raman: $\tilde{\nu}$ = 2951, 1505, 1421, 1176, 931, 888, 708, 561, 524 cm^{-1}. m/z (ESI^+-MS): 101.85 $[M\text{-}N_5]^+$. IS: >40 J. FS: >360 N. 1H NMR (500 MHz, DMSO-d6) δ 8.74 (d, J = 125.8 Hz, 4H), 7.70 (s, 1H), 7.34 (s, 1H), 3.35 (s, 2H). Elemental analysis (%) calcd. for $C_3H_8N_8O$ (172.17): C, 20.93; H, 4.69; N, 65.09; O, 9.29; found: C, 21.05; H, 4.54; N, 65.03; O, 9.38.

Glycine pentazolate (7): Dispersed 1.05 mmol of pentazolate silver salt in a mixed solution of methanol and water in a ratio of 9:1. Added 1.00 mmol of water solution of methylamine hydrochloride to the above mixed solution. The reaction was stirred at room temperature for 6 hours under dark conditions. Filtered to remove silver chloride precipitate, and dried the filtrate under reduced pressure to obtain a white solid. Yield:128.5 mg (0.88 mmol, 88%). Td (onset): 116 °C. IR: $\tilde{\nu}$ = 3146, 2921, 2590, 1734, 1577, 1503, 1407, 1254, 1221, 1120, 1042, 889, 646, 492 cm^{-1}. Raman: $\tilde{\nu}$ = 2977, 1750, 1260, 1179, 1112, 1047, 868, 646 cm^{-1}. m/z (ESI^+-MS): 75.85 $[M\text{-}N_5]^+$. IS: >40 J. FS: >360 N. 1H NMR (500 MHz, DMSO-d6) δ 8.31 (s, 3H), 3.50 (s, 2H). Elemental analysis (%) calcd. for $C_2H_6N_6O_2$ (146.13): C, 16.44; H, 4.14; N, 57.52; O, 21.90; found: C, 16.13; H, 4.36; N, 57.82; O, 21.69.

2. IR, Raman and ^{1}H NMR spectrum

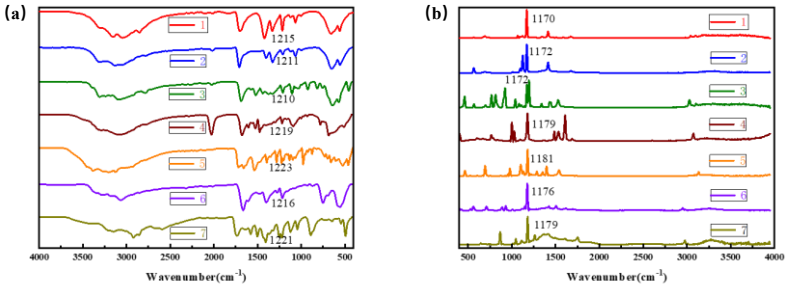

Figure S1. (a) IR spectra and (b) Raman spectra of compound 1−7

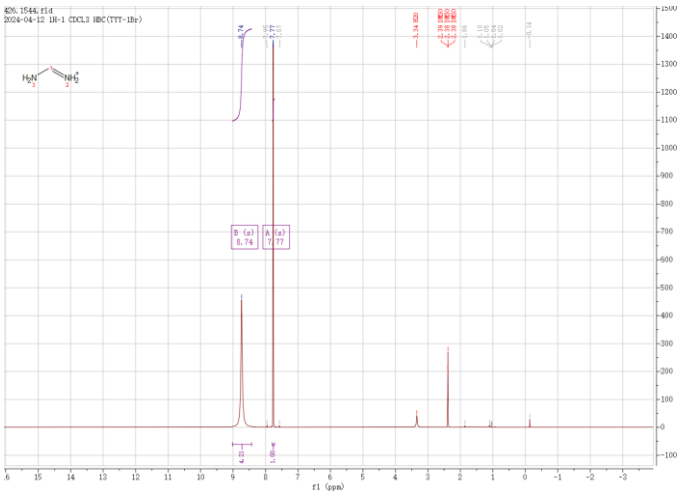

Figure S2. ^{1}H NMR analysis of compound 1

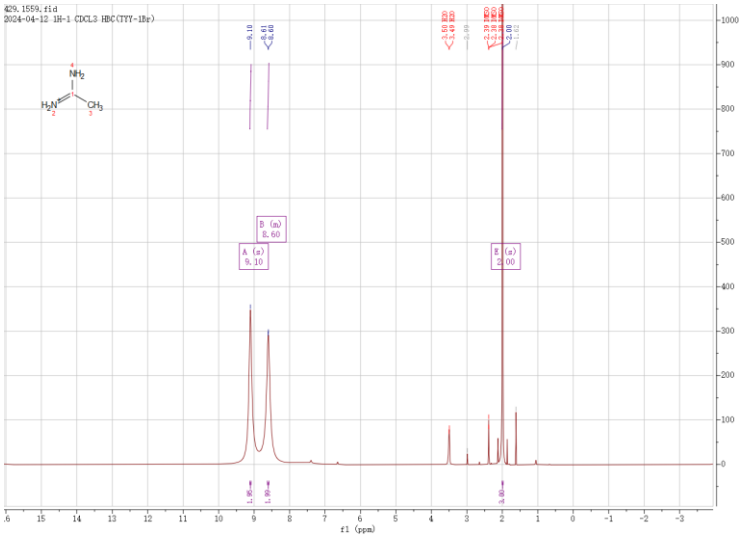

Figure S3. ^{1}H NMR analysis of compound 1

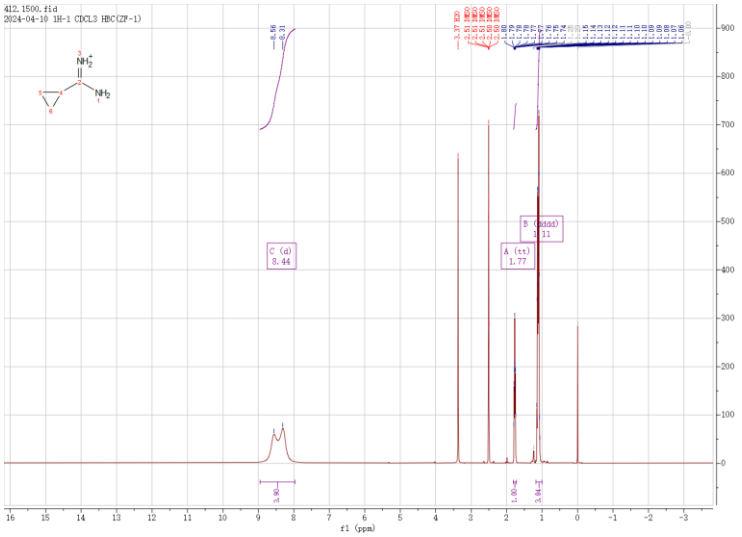

Figure S4. ^{1}H NMR analysis of compound 3

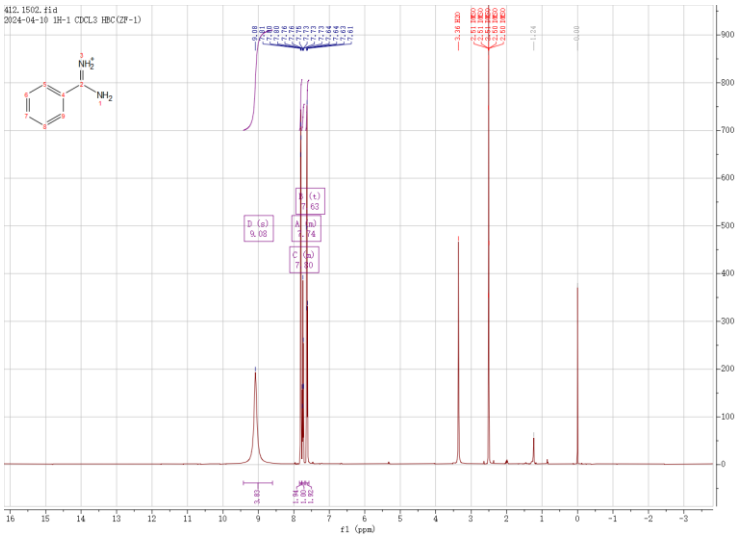

Figure S5. ^{1}H NMR analysis of compound 4

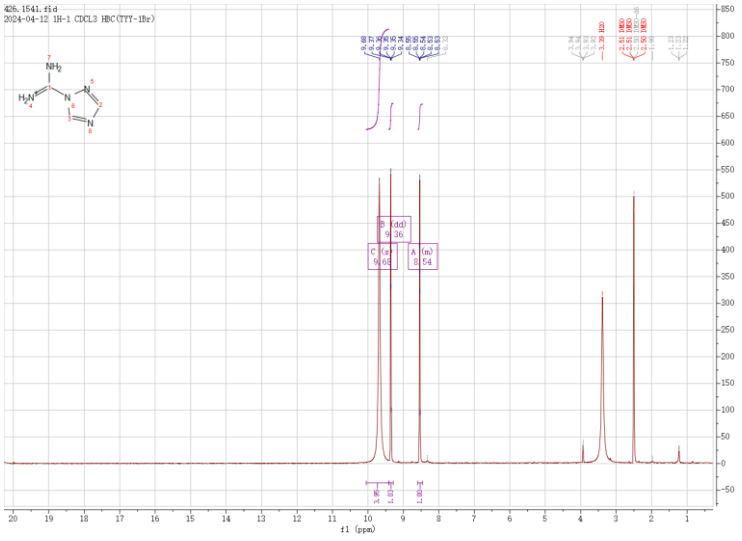

Figure S6. ^{1}H NMR analysis of compound 5

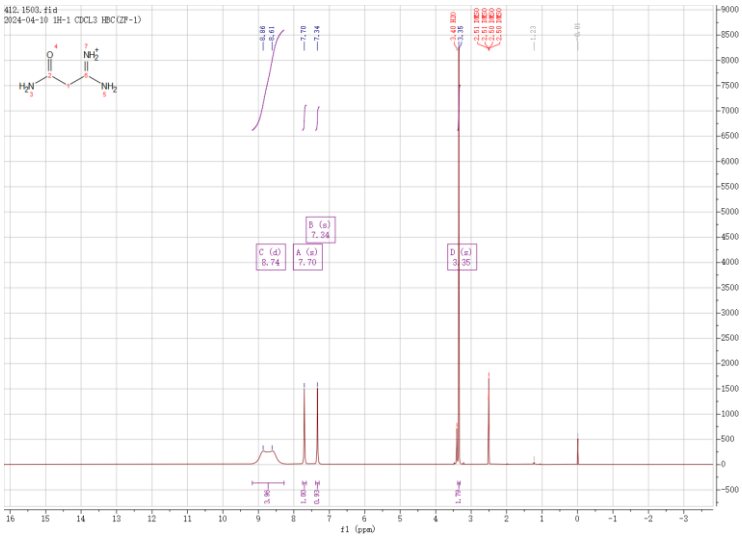

Figure S7. ^{1}H NMR analysis of compound 6

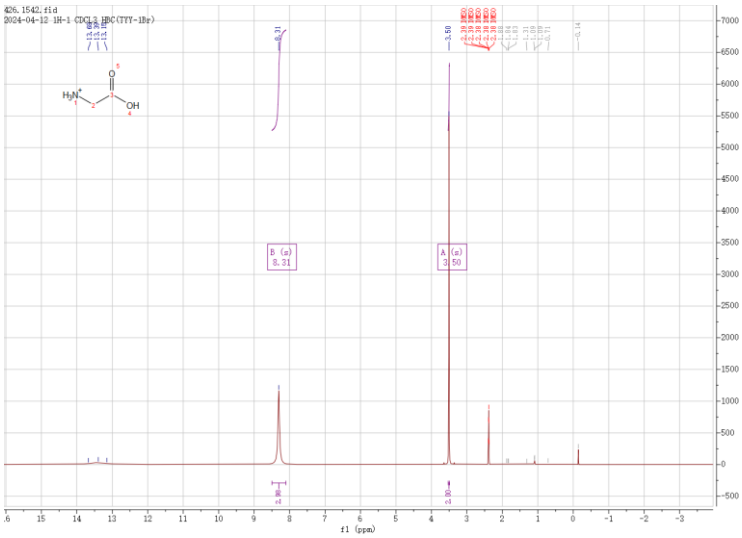

Figure S8. ^{1}H NMR analysis of compound 7

3. Crystal structure data

Table S1. Crystal data and structure refinement for 1-4

Crystal	1	2	3	4
CCDC number	2322435	2322436	2322437	2322438
Empirical formula	CH5N7	C2H7N7	C4H9N7	C7H9N7
Formula weight	115.12	129.125	155.163	191.21
Temperature [K]	296(2)	273.15	273.15	296(2)
Crystal system	monoclinic	orthorhombic	monoclinic	triclinic
Space group (number)	$C2/c$ (15)	$Pnma$ (62)	$P2_1/m$ (11)	$P\bar{1}$ (2)
a [Å]	4.9752(6)	13.629(1)	7.0037(15)	3.9161(5)
b [Å]	15.7038(18)	6.5997(6)	7.0175(15)	9.7152(11)
c [Å]	7.0385(10)	7.4672(5)	7.7191(16)	12.5718(14)
α [°]	90	90	90	84.813(3)
β [°]	107.756(4)	90	96.937(7)	86.135(4)
γ [°]	90	90	90	83.993(4)
Volume [Å^3]	523.72(12)	671.65(9)	376.60(14)	472.92(10)
Z	4	4	2	2
ρ_{calc} [gcm^{-3}]	1.460	1.277	1.368	1.343
μ [mm^{-1}]	0.116	0.098	0.100	0.094
F(000)	240	272.210	164.119	200
Crystal size [mm^3]	0.180×0.170×0.160	0.22×0.2×0.19	0.4×0.2×0.2	0.200×0.030×0.010
Crystal colour	colourless	colourless	colourless	colourless
Crystal shape	block	plate	block	needle
Radiation	MoKα (λ=0.71073 Å)	Mo Kα (λ=0.71073 Å)	Mo Kα (λ=0.71073 Å)	MoKα (λ=0.71073 Å)
2θ range [°]	5.19 to 54.86 (0.77 Å)	6.22 to 54.90 (0.77 Å)	5.32 to 50.12 (0.84 Å)	4.23 to 55.13 (0.77 Å)
Index ranges	−6 ≤ h ≤ 5 −20 ≤ k ≤ 20 −8 ≤ l ≤ 9	−14 ≤ h ≤ 17 −8 ≤ k ≤ 8 −8 ≤ l ≤ 9	−8 ≤ h ≤ 7 −8 ≤ k ≤ 8 −8 ≤ l ≤ 9	−5 ≤ h ≤ 5 −12 ≤ k ≤ 12 0 ≤ l ≤ 16
Reflections collected	2234	5669	5041	2115
Independent reflections	596 Rint = 0.0258 Rsigma = 0.0253	836 Rint = 0.0333 Rsigma = 0.0244	727 Rint = 0.1434 Rsigma = 0.0714	2115 Rint = ? Rsigma = 0.0510
Completeness to θ = 22.734°	98.3 %	99.6 %	99.3 %	97.7 %
Data/Restraints/Parameters	596/0/38	836/0/62	727/1/87	2115/0/128

Goodness-of-fit on F^2	1.090	1.0424	1.0564	1.043
Final R indexes [$I \geq 2\sigma(I)$]	R1 = 0.0341 wR2 = 0.0805	R1 = 0.0444 wR2 = 0.1078	R1 = 0.0580 wR2 = 0.1201	R1 = 0.0547 wR2 = 0.1222
Final R indexes [all data]	R1 = 0.0453 wR2 = 0.0855	R1 = 0.0687 wR2 = 0.1230	R1 = 0.0881 wR2 = 0.1406	R1 = 0.0969 wR2 = 0.1373
Largest peak/hole [eÅ^{-3}]	0.16/-0.13	0.22/-0.22	0.35/-0.37	0.17/-0.17

Table S2. Crystal data and structure refinement for 5-7

Crystal	5	6	7
CCDC number	2322439	2322440	2322441
Empirical formula	$C_3H_8N_{10}O$	$C_3H_8N_8O$	$C_2H_6N_6O_2$
Formula weight	200.19	172.17	146.13
Temperature [K]	273.15	273.15	273.15
Crystal system	monoclinic	monoclinic	triclinic
Space group (number)	$P2_1/c$ (14)	$P2_1/c$ (14)	$P\bar{1}$ (2)
a [Å]	6.450(5)	4.8465(4)	5.2112(15)
b [Å]	12.008(10)	9.6906(7)	7.849(2)
c [Å]	12.141(11)	16.5974(12)	7.880(3)
α [°]	90	90	78.116(9)
β [°]	102.19(3)	92.765(2)	76.103(10)
γ [°]	90	90	73.730(9)
Volume [Å^3]	919.0(13)	778.60(10)	297.01(16)
Z	4	4	2
ρ_{calc} [gcm^{-3}]	1.447	1.469	1.634
μ [mm^{-1}]	0.117	0.118	0.141
F(000)	416	360	152
Crystal size [mm^3]	0.18×0.12×0.11	0.13×0.12×0.11	0.3×0.2×0.2
Crystal colour	light colourless	colourless	colourless
Crystal shape	block	block	block
Radiation	MoK_α (λ=0.71073 Å)	MoK_α (λ=0.71073 Å)	MoK_α (λ=0.71073 Å)
2θ range [°]	4.83 to 48.60 (0.86 Å)	4.87 to 50.05 (0.84 Å)	5.39 to 49.98 (0.84 Å)
Index ranges	$-7 \leq h \leq 6$ $-13 \leq k \leq 12$ $-10 \leq l \leq 14$	$-5 \leq h \leq 5$ $-10 \leq k \leq 11$ $-19 \leq l \leq 19$	$-6 \leq h \leq 6$ $-9 \leq k \leq 9$ $-9 \leq l \leq 9$
Reflections collected	3729	6507	2455
Independent reflections	1478 R_{int} = 0.0800 R_{sigma} = 0.1197	1376 R_{int} = 0.0541 R_{sigma} = 0.0461	1030 R_{int} = 0.0265 R_{sigma} = 0.0327
Completeness to	98.7 %	99.9 %	97.7 %

θ = 24.302°			
Data/ Restraints / Parameters	1478/0/130	1376/0/109	1030/0/115
Goodness-of-fit on F^2	1.034	1.040	1.080
Final R indexes	R_1 = 0.0625	R_1 = 0.0404	R_1 = 0.0315
[$I \geq 2\sigma(I)$]	wR_2 = 0.1120	wR_2 = 0.0929	wR_2 = 0.0833
Final R indexes	R_1 = 0.1410	R_1 = 0.0573	R_1 = 0.0346
[all data]	wR_2 = 0.1341	wR_2 = 0.1013	wR_2 = 0.0855
Largest peak/hole [eÅ^{-3}]	0.21/-0.28	0.23/-0.26	0.20/-0.16

Tab S3. Bond length of pentazole formamidine

Parameter	Bond length(Å)	Parameter	Bond length(Å)
N1-N2	1.318(3)	N3-N3	1.323(4)
N2-N3	1.312(4)	N4-C1	1.294(3)

Tab S4. Bond angle of pentazole formamidine

Parameter	Bond angle(o)	Parameter	Bond angle(o)
N2-N1-N2	108.2(3)	N2-N3-N3	108.1(13)
N3-N2-N1	107.8(2)	N4-C1-N4	125.2(5)

Table S5. Torsion angle of pentazole formamidine

Parameter	Torsion angle(°)	Parameter	Torsion angle(°)
N1-N2-N3-N3	−0.8(3)	N2-N1-N2-N3	-0.32(12)

Table S6. Bond length of pentazole acetamidine

Parameter	Bond length(Å)	Parameter	Bond length(Å)
N1-N5	1.302(4)	N4-N5	1.306(4)
N1-N2	1.313(4)	N6-C2	1.296(4)
N2-N3	1.297(4)	C1-C2	1.486(5)
N3-N4	1.313(4)	C2-N7	1.295(4)

Table S7. Bond angle of pentazole acetamidine

Parameter	Bond angle(o)	Parameter	Bond angle(o)
N5-N1-N2	108.4(2)	N1-N5-N4	107.6(2)
N3-N2-N1	107.8(3)	N7-C2-N6	121.7(3)
N2-N3-N4	108.1(3)	N7-C2-C1	119.5(3)
N5-N4-N3	108.1(3)	N6-C2-C1	118.8(3)

Table S8. Torsion angle of pentazole acetamidine

Parameter	Torsion angle(°)	Parameter	Torsion angle(°)

N4-N3-N2-N1	−0.14(2)	C1-C2-N6-N7	178.95(3)
N3-N4-N5-N1	−0.10(2)	N6-N7-C1-C2	178.92(3)
N6-C3-C2-N7	178.95(3)	N5-N4-N3-N2	0.12(2)
N2-N1-N5-N4	0.00(2)	N5-N1-N2-N3	0.10(2)

Table S9. Bond length of pentazole cyclopropane-1-carboxi-midamide

Parameter	Bond length(Å)	Parameter	Bond length(Å)
N1-N2	1.302(4)	N7-C1	1.304(4)
N1-N5	1.305(4)	C1-C2	1.456(5)
N2-N3	1.314(4)	C2-C3	1.505(3)
N3-N4	1.312(4)	C2-C3	1.505(3)
N4-N5	1.309(4)	C3-C3	1.470(5)
N6-C1	1.316(4)		

Table S10. Bond angle of pentazole cyclopropane-1-carboxi-midamide

Parameter	Bond angle(°)	Parameter	Bond angle(°)
N2-N1-N5	108.6(3)	N7-C1-C2	118.7(3)
N1-N2-N3	107.5(3)	N6-C1-C2	121.0(3)
N4-N3-N2	108.3(3)	C1-C2-C3	120.3(2)
N5-N4-N3	107.4(3)	C1-C2-C3	120.3(2)
N1-N5-N4	108.2(3)	C3-C2-C3	58.5(2)
N7-C1-N6	120.3(3)	C3-C3-C2	60.76(11)

Table S11. Torsion angle of pentazole cyclopropane-1-carboxi-midamide

Parameter	Torsion angle(°)	Parameter	Torsion angle(°)
N4-N3-N2-N1	−0.14(11)	C3-C3-C2-C1	−109.10(11)
N3-N4-N5-N1	−0.1(3)	C1-C2-N7-N6	180.00(4)
N6-C2-C2-C3	34.46(11)	N5-N4-N3-N2	0.12(2)
N2-N1-N5-N4	0.00(2)	N5-N1-N2-N3	0.10(2)
N7-C1-C2-C3	−145.54(11)	C3-C3-N6-N7	89.40(11)

Table S12. Bond length of pentazole Benzamidine

Parameter	Bond length(Å)	Parameter	Bond length(Å)
N1-N5	1.318(6)	C1-C2	1.470(7)
N1-N2	1.330(6)	C2-C3	1.383(7)
N2-N3	1.322(7)	C2-C7	1.392(7)
N3-N4	1.302(6)	C3-C4	1.391(8)
N4-N5	1.317(6)	C4-C5	1.350(9)
N6-C1	1.295(6)	C5-C6	1.363(8)
N7-C1	1.311(6)	C6-C7	1.372(8)

Table S13. Bond angle of pentazole Benzamidine

Parameter	Bond angle(°)	Parameter	Bond angle(°)
N5-N1-N2	107.4(4)	C3-C2-C7	119.3(5)
N3-N2-N1	107.9(4)	C3-C2-C1	120.1(5)
N4-N3-N2	107.9(4)	C7-C2-C1	120.6(5)
N3-N4-N5	108.9(4)	C2-C3-C4	118.5(6)
N4-N5-N1	108.0(4)	C5-C4-C3	121.5(6)
N6-C1-N7	121.8(5)	C4-C5-C6	120.2(6)
N6-C1-C2	119.5(4)	C5-C6-C7	120.0(6)
N7-C1-C2	118.7(4)	C6-C7-C2	120.4(5)

Table S14. Bond length of pentazole 1H-1,2,4-triazole-1-carboxamidine

Parameter	Bond length(Å)	Parameter	Bond length(Å)
N1-N5	1.311(3)	N4-N5	1.321(2)
N1-N2	1.313(2)	N6-C2	1.357(2)
N2-N3	1.313(2)	N7-C1	1.309(2)
N3-N4	1.314(2)	C1-N8	1.299(2)

Table S15. Bond angle of pentazole 1H-1,2,4-triazole-1-carboxamidine

Parameter	Bond angle(°)	Parameter	Bond angle(°)
N5-N1-N2	108.14(16)	N1-N5-N4	108.17(16)
N3-N2-N1	107.85(16)	N7-C1-N6	118.06(16)
N2-N3-N4	108.43(15)	N10-C2-N6	110.14(17)
N5-N4-N3	107.42(16)	N9-C3-N10	115.20(19)

Table S16. Torsion angle of pentazole 1H-1,2,4-triazole-1-carboxamidine

Parameter	Torsion angle(°)	Parameter	Torsion angle(°)
N4-N3-N2-N1	0.00(2)	C3-N10-C2-N6	−0.10(2)
N3-N4-N5-N1	0.10(2)	C2-N6-N9-C3	0.70(2)
C1-N6-N9-C3	177.40(16)	C2-N6-C1-N7	−15.40(3)
N2-N1-N5-N4	−0.10(2)	C2-N6-C1-N8	164.97(18)
C1-N6-C2-N10	−176.52(17)	C2-N10-C3-N9	0.70(3)

Table S17. Bond length of pentazole 3-amino-3-iminopropanamide

Parameter	Bond length(Å)	Parameter	Bond length(Å)
O1-C1	1.229(2)	N8-C3	1.298(2)
N4-N3	1.306(2)	N7-C3	1.309(2)
N4-N5	1.324(2)	C3-C2	1.496(2)
N1-N2	1.311(2)	N6-C1	1.321(2)
N1-N5	1.309(2)	C2-C1	1.521(2)
N3-N2	1.328(2)		

Table S18. Bond angle of pentazole 3-amino-3-iminopropanamide

Parameter	Bond angle(°)	Parameter	Bond angle(°)
N3-N4-N5	107.92(15)	N7-C3-C2	117.75(15)
N5-N1-N2	108.52(15)	N1-N5-N4	107.90(14)
N4-N3-N2	108.18(14)	C3-C2-C1	111.26(13)
N1-N2-N3	107.48(14)	O1-C1-N6	123.89(16)
N8-C3-N7	121.89(16)	O1-C1-C2	120.31(15)
N8-C3-C2	120.36(15)	N6-C1-C2	115.75(15)

Table S19. Torsion angle of pentazole 3-amino-3-iminopropanamide

Parameter	Torsion angle(°)	Parameter	Torsion angle(°)
N4-N3-N2-N1	−0.14(19)	C3-C2-C1-O1	−34.60(2)
N3-N4-N5-N1	−0.10(2)	C3-C2-C1-N6	147.71(15)
N8-C3-C2-C1	113.56(17)	N5-N4-N3-N2	0.12(19)
N2-N1-N5-N4	0.00(2)	N5-N1-N2-N3	0.10(2)
N7-C3-C2-C1	−67.14(19)		

Table S20. Bond length of pentazole glycine

Parameter	Bond length(Å)	Parameter	Bond length(Å)
O1-C2	1.210(18)	N1-N2	1.315(17)
C1-C2	1.510(18)	N4-N5	1.311(18)
C1-N6	1.469(18)	N3-N2	1.309(17)
C2-O2	1.314(16)	N3-N4	1.315(17)
N1-N5	1.310(17)		

Table S21. Bond angle of pentazole glycine

Parameter	Bond angle(°)	Parameter	Bond angle(°)
N2-N3-N4	108.25(11)	O2-C2-C1	116.51(11)
N5-N4-N3	107.83(11)	O1-C2-O2	121.82(11)
N5-N1-N2	108.24(12)	O1-C2-C1	121.66(12)
N3-N2-N1	107.68(11)	N6-C1-C2	110.40(11)
N1-N5-N4	108.00(11)		

Table S22. Torsion angle of pentazole glycine

Parameter	Torsion angle(°)	Parameter	Torsion angle(°)
N4-N3-N2-N1	0.04(14)	N6-C1-C2-O1	−1.21(17)
N3-N4-N5-N1	0.18(15)	N5-N4-N3-N2	-0.15(15)
N2-N3-N4-N5	-0.14(15)	N5-N1-N2-N3	0.07(15)
N6-C1-C2-O2	177.91(11)		

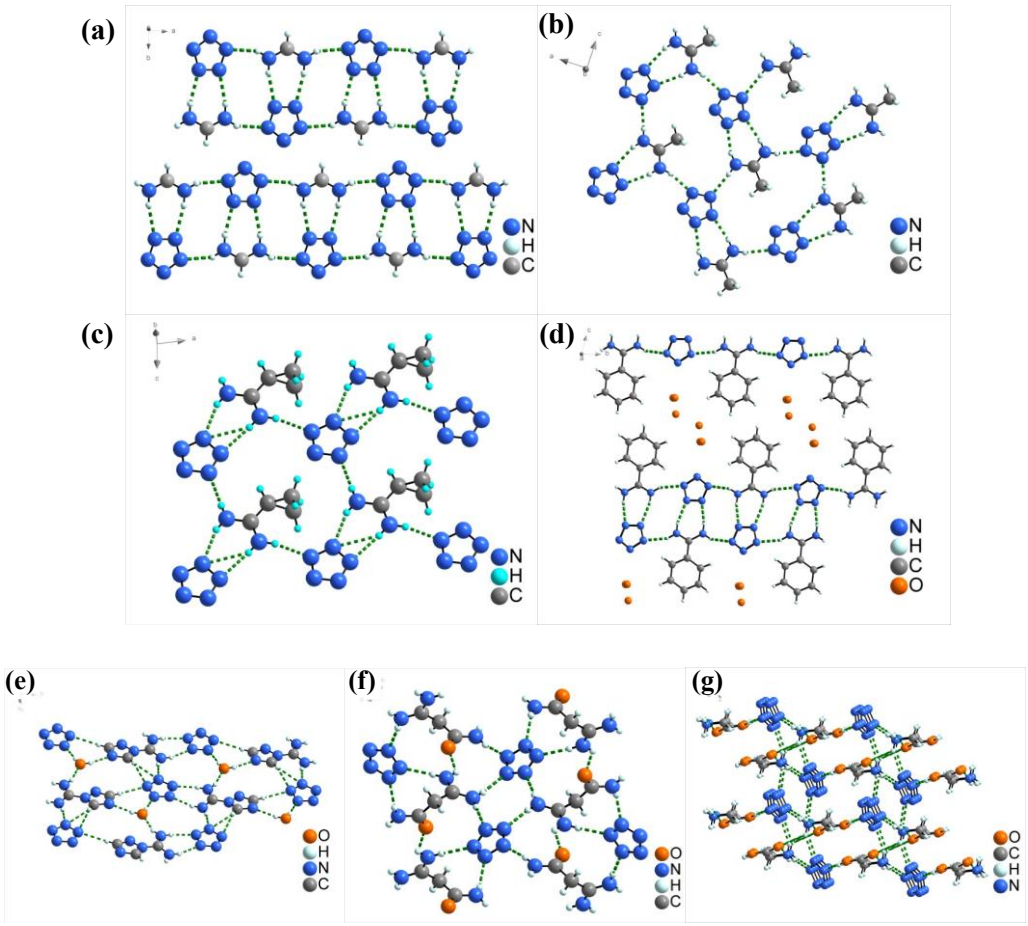

Figure S9. Intramolecular hydrogen bonds of compound 1-7

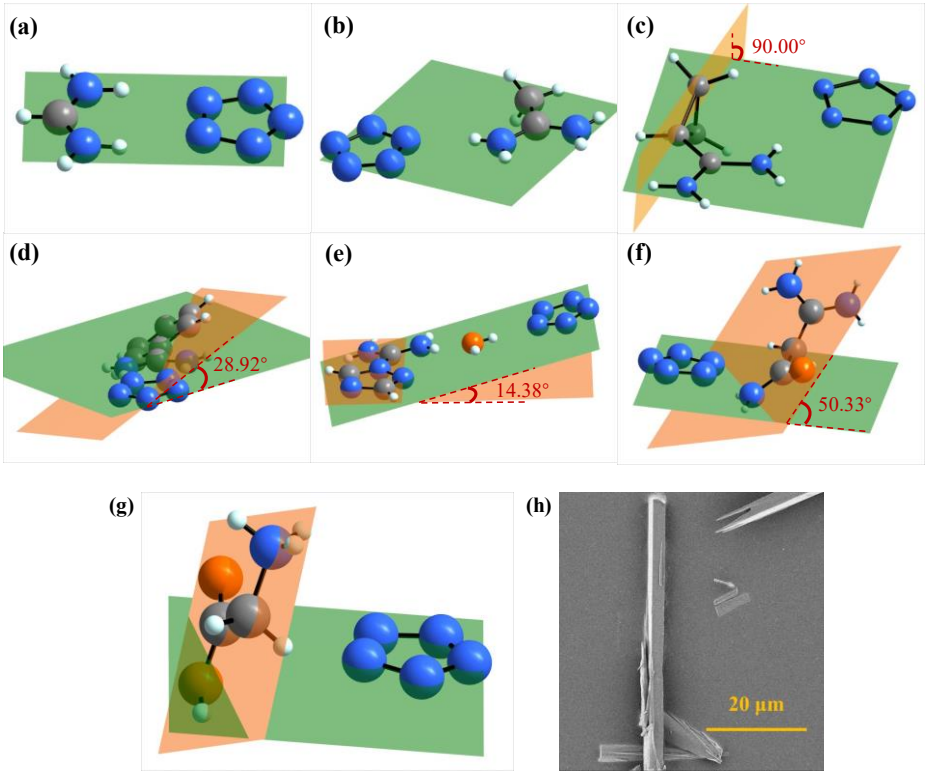

Figure S10. (a-g) Dihedral angle of compound1-7 and (h) SEM of 7

4. TG analysis

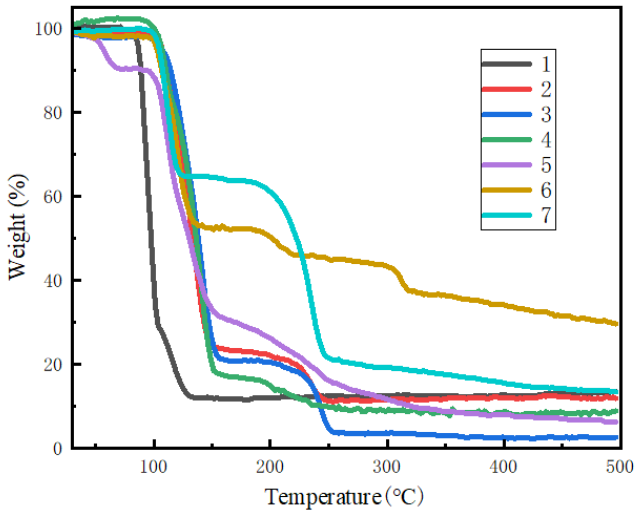

Figure S11. TG of compound 1−7

5. ESP and NCI analysis

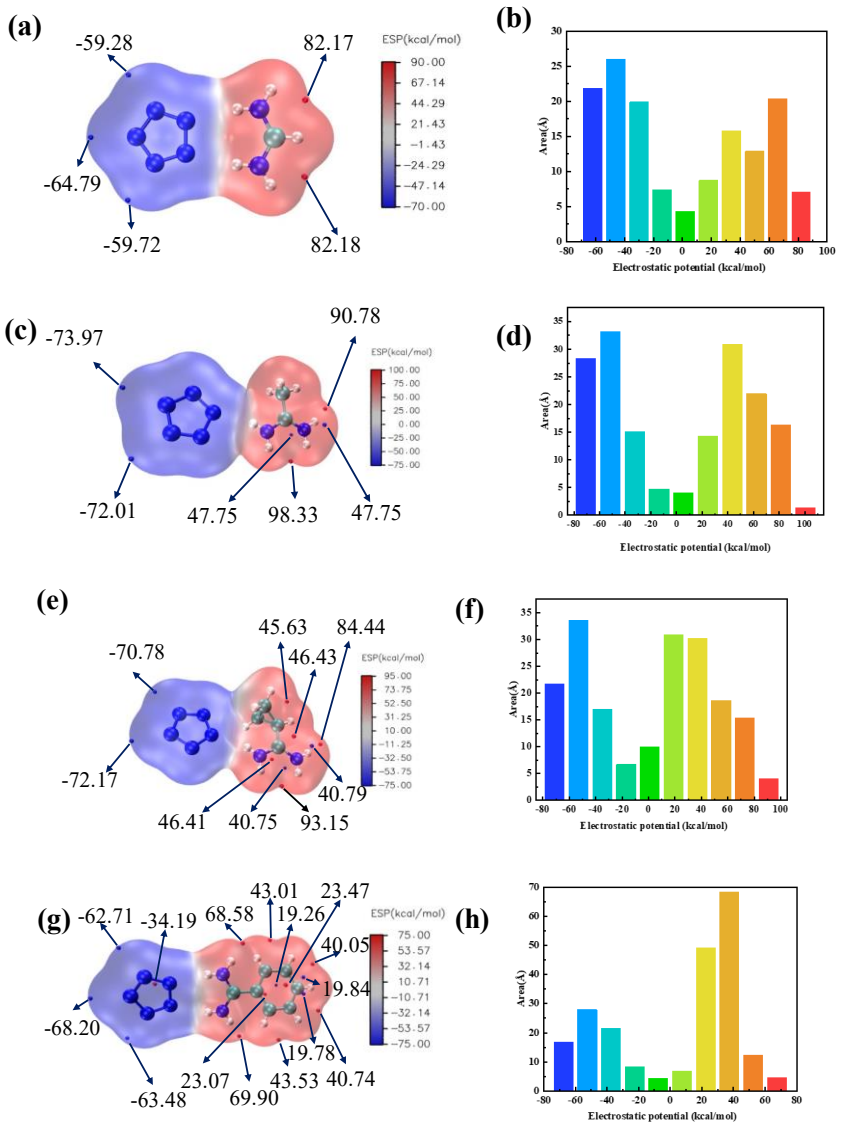

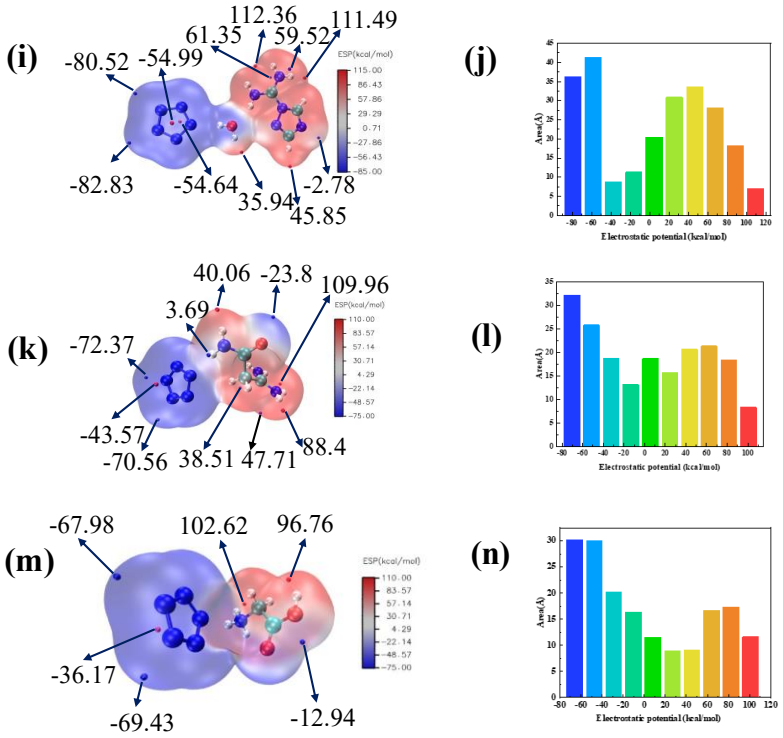

Figure S12. ESP-mapped molecular van der Waals (vdW) surfaces of the structurally optimized molecules (Surface local ESP minima and maxima are represented as blue and red spheres, respectively) and vdW surface areas for each ESP range for compound 1-7

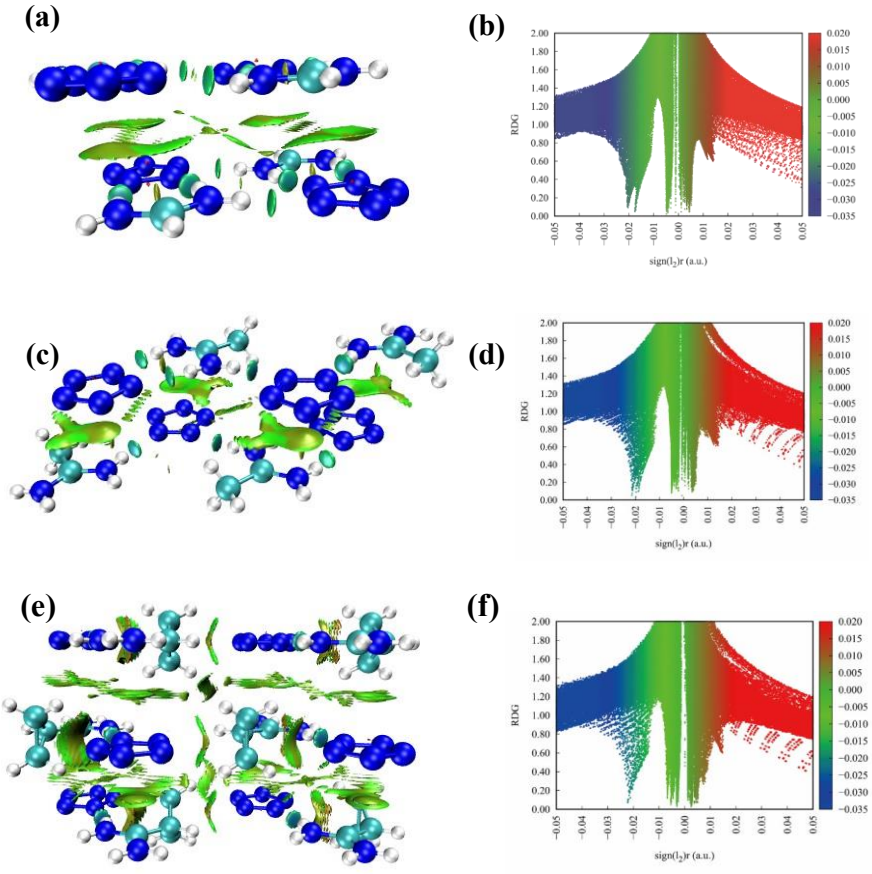

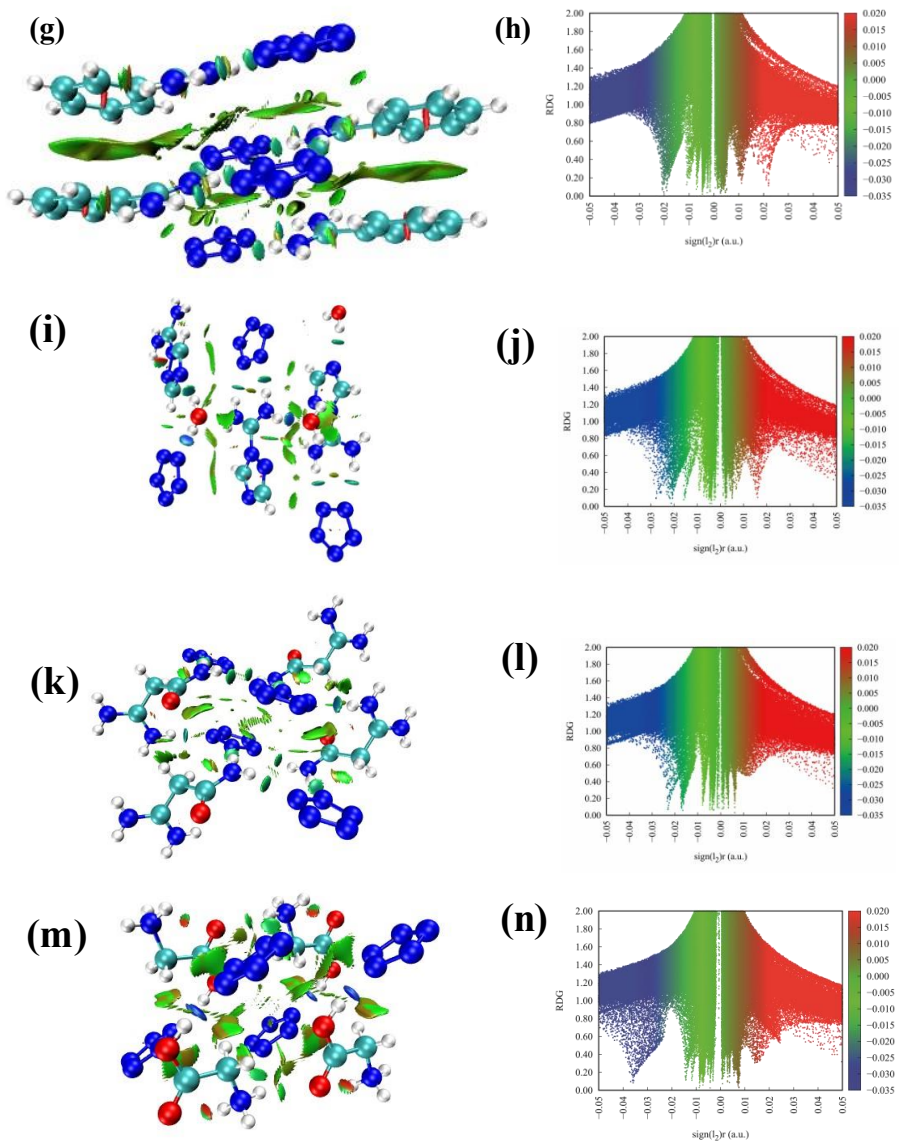

Figure S13. Noncovalent interaction analyses and scatter graphs for 1-7 (including hydrogen bonds and π−π interactions, blue: strong attraction; green: weak interaction; red: strong repulsion)

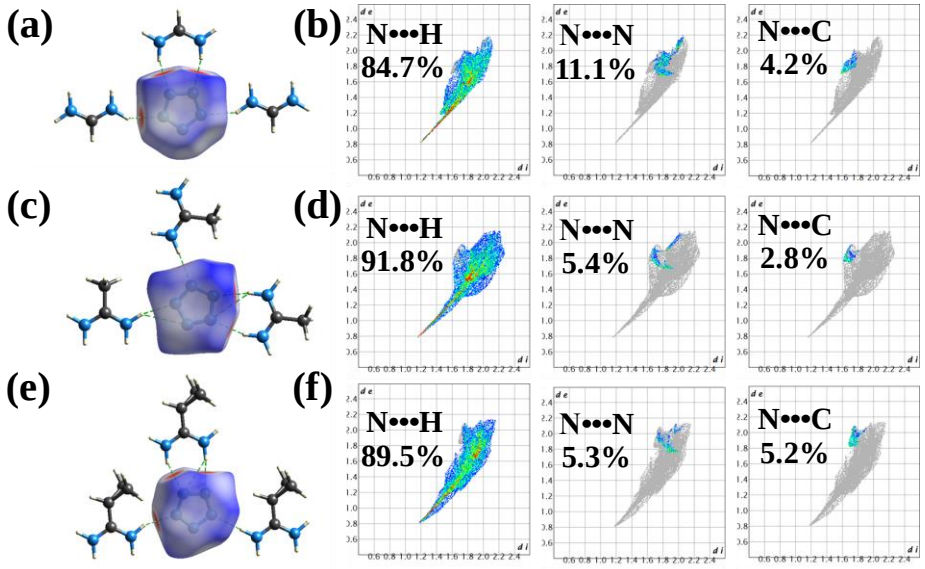

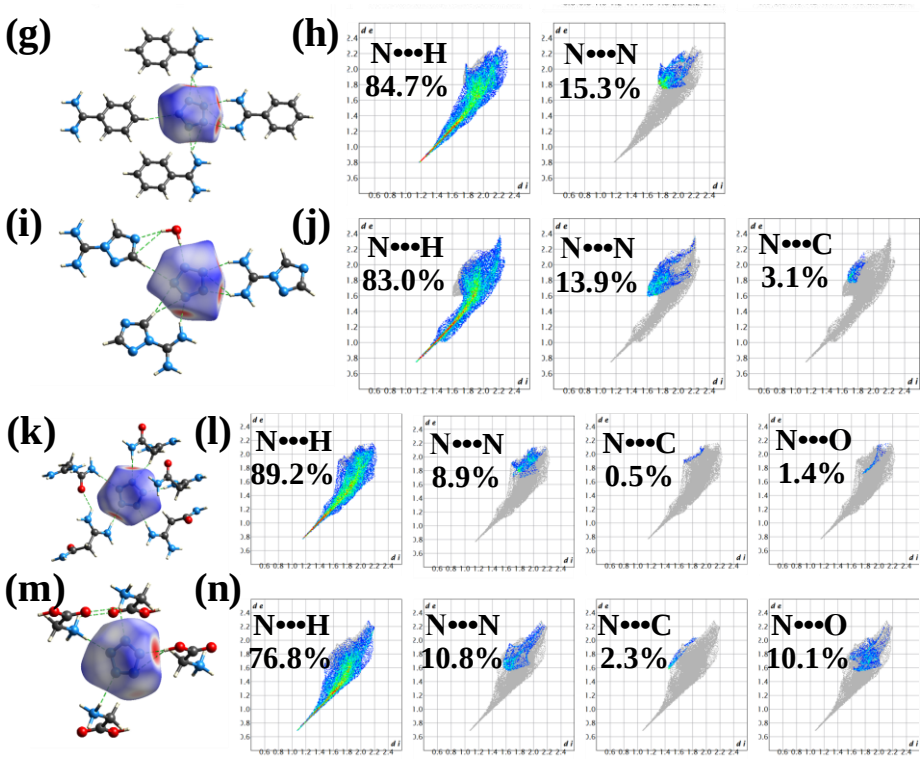

Figure S14. Hirshfeld surface and 2D fingerprint plots in crystal stacking of cyclo-N_5^- of (a, b) compound 1, (c, d) compound 2, (e, f) compound 3, (g, h) compound 4, (i, j) compound 5, (k, l) compound 6, (m, n) compound 7.

6. Physicochemical and Energetic Properties

For energetic salts, the solid-phase heats of formation are calculated on the basis of a Born-Haber energy cycle (Scheme S1).

Based on a Born-Haber energy cycle, the heat of formation of a salt can be simplified by the formula given in Equation (1):

$$\Delta H_f(\text{salt, 298K}) = \Delta H_f(\text{cation, 298K}) + \Delta H_f(\text{anion, 298K}) - \Delta H_L \quad (1)$$

where ΔH_L is the lattice energy of the salts, which could be predicted by using the formula suggested by Jenkins et al[8-10]. [Eq. (2)]

$$\Delta H_L = U_{POT} + [\, p(n_M/2 - 2) + q(n_X/2 - 2)]RT \quad (2)$$

where n_M and n_X depend on the nature of the ions, M_{p+} and X_{q-}, and are equal to 3 for monatomic ions, 5 for linear polyatomic ions, and 6 for nonlinear polyatomic ions.

The equation for lattice potential energy UPOT [Eq. (3)] has the form:

$$U_{POT}\ (\text{kJ·mol}^{-1}) = \gamma\ (\rho_m/M_m)^{1/3} + \delta \quad (3)$$

Where ρ_m/g·cm^{-3} is the density, M_m is the chemical formula mass of the ionic material, and values for the coefficients γ/ kJ·mol^{-1} cm and δ/kJ·mol^{-1} are taken from the literature[11].

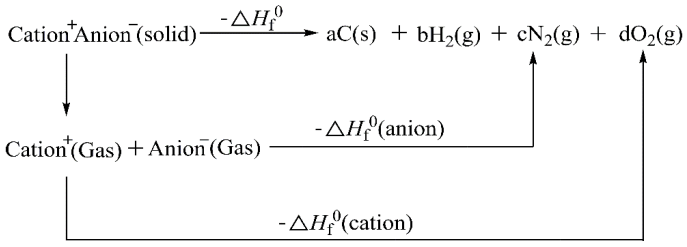

Scheme S1. Born-Haber cycle for the formation of ionic salts.

At the B3LYP/6-311+G** level[12-15], geometric optimization and frequency analysis were carried out for cations in all compounds, and the stable structures at the local energy minimum on the potential energy surface were obtained without imaginary frequencies. The enthalpy of formation of the cation section was calculated based on the designed isodesmic reaction. The enthalpy of formation of pentazolate anion has been reported in relevant literature[16].

At 298 K, the standard heat of formation of cations can be calculated by the following equation[17, 18]:

$$\Delta H\ (\text{cation, 298K}) = \Delta E\ (\text{cation, 298K}) + \Delta(PV) = \Delta E_0 + \Delta ZPE + \Delta H_T + \Delta nRT$$

where ΔE_0 is the difference in total energies between the products and reactants at 0 K, ΔZPE is the difference in zero energy between the product and reactant at 0 K, and ΔHT is the temperature correction factor. As shown in **Scheme S2.**, the following is the isodesmic reactions for all the calculated cations. The heat of formation of small molecules can be found in the literature or calculated with G4.

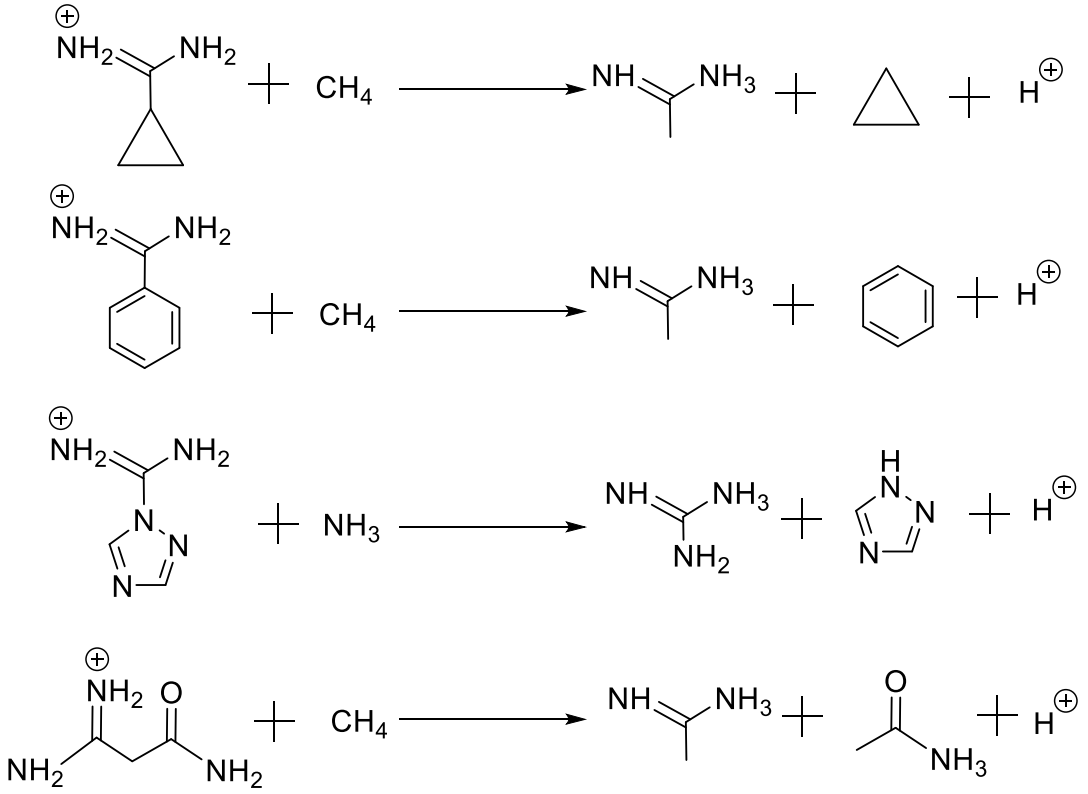

Scheme S2. Isodesmic reactions for all the calculated cations.

Table S23. Heat of formation

Compound	ΔH_c[a](anion) (kJ·mol^{-1})	ΔH_c[b] (cation) (kJ·mol^{-1})	ΔH_L[c] (kJ·mol^{-1})
1	258.70	621.35	567.98
2	258.70	552.42	533.11
3	258.70	653.27	516.80
4	258.70	695.00	480.43
5	258.70	862.00	502.83
6	258.70	476.76	508.60
7	258.70	265.31	550.57

a. Heat of formation. b. Heat of formation. c. Lattice energy.

7. References

1. M. J. Frisch, G. W. Trucks, H. B. Schlegel, G. E. Scuseria, M. A. Robb, J. R. Cheeseman, G. Scalmani, V. Barone, B. Mennucci and G. A. Petersson, in *Gaussian 09*, Gaussian Inc Wallingford, 2009.
2. E. R. Johnson, S. Keinan, P. Mori-Sánchez, J. Contreras-García, A. J. Cohen and W. Yang, *J. Am. Chem. Soc.*, 2010, **132**, 6498-6506.
3. J. Zhang and T. Lu, *Phys. Chem. Chem. Phys.*, 2021, **23**, 20323-20328.
4. W. Humphrey, A. Dalke and K. Schulten, *J. Mol. Graphics*, 1996, **14**, 33-38.
5. T. Lu and F. Chen, *J. Comput. Chem.*, 2012, **33**, 580-592.
6. Z. Liu, T. Lu and Q. Chen, *Carbon*, 2021, **171**, 514-523.
7. P. R. Spackman, M. J. Turner, J. J. McKinnon, S. K. Wolff, D. J. Grimwood, D. Jayatilaka and M. A. Spackman, *J. Appl. Crystallogr.*, 2021, **54**, 1006-1011.
8. H. D. B. Jenkins, D. Tudela and L. Glasser, *Inorg. Chem.*, 2002, **41**, 2364-2367.
9. H. D. B. Jenkins, *Journal of Chemical Education*, 2005, **82**, 950.
10. E. F. C. Byrd and B. M. Rice, *The Journal of Physical Chemistry A*, 2009, **113**, 345-352.
11. H. D. B. Jenkins, H. K. Roobottom, J. Passmore and L. Glasser, *Inorg. Chem.*, 1999, **38**, 3609-3620.
12. P. J. Stephens, F. J. Devlin, C. F. Chabalowski and M. J. Frisch, *J. Phys. Chem. C*, 1994, **98**, 11623-11627.
13. K. Raghavachari, *Theor. Chem. Acc.*, 2000, **103**, 361-363.
14. J. A. Pople, J. S. Binkley and R. Seeger, *International Journal of Quantum Chemistry*, 1976, **10**, 1-19.
15. P. C. Hariharan and J. A. Pople, *Theor. Chem. Acc.*, 1973, **28**, 213-222.
16. K. O. Christe, D. A. Dixon, M. Vasiliu, R. Haiges and B. Hu, *Propellants, Explosives, Pyrotechnics*, 2019, **44**, 263-266.
17. Y. Tang, Z. Yin, A. K. Chinnam, R. J. Staples and J. n. M. Shreeve, *Inorg. Chem.*, 2020, **59**, 17766-17774.
18. V. Thaltiri, R. J. Staples and J. n. M. Shreeve, *Journal of Materials Chemistry A*, 2024, DOI: 10.1039/D4TA03084B.